Analysis of Fe-doped ZnO thin films for degradation of rhodamine B, methylene blue, and Escherichia coli under visible light

by Eko Hidayanto

Submission date: 12-May-2022 08:10AM (UTC+0700)
Submission ID: 1834229370
File name: C3.pdf (1.25M)
Word count: 5570
Character count: 28184

Materials Research Express

PAPER · **OPEN ACCESS**

Analysis of Fe-doped ZnO thin films for degradation of rhodamine b, methylene blue, and *Escherichia coli* under visible light

To cite this article: Heri Sutanto *et al* 2021 *Mater. Res. Express* **8** 116402

IOP Publishing Mater. Res. Express 8 (2021) 116402 https://doi.org/10.1088/2053-1591/ac33fe

Materials Research Express

PAPER

Analysis of Fe-doped ZnO thin films for degradation of rhodamine b, methylene blue, and *Escherichia coli* under visible light

Heri Sutanto[1,2], **Ilham Alkian**[2,3], **Mukholit Mukholit**[1], **Arsyadio Aditya Nugraha**[1], **Eko Hidayanto**[1], **Indras Marhaendrajaya**[1] **and Priyono Priyono**[1]

[1] Department of Physics, Faculty of Science and Mathematics, Diponegoro University, Jawa Tengah 50275, Indonesia
[2] Smart Materials Research Center (SMARC), Diponegoro University, Jawa Tengah 50275, Indonesia
[3] Graduate Program of Environmental Science, School of Postgraduate Studies, Diponegoro University, Jawa Tengah 50241, Indonesia

E-mail: herisutanto@live.undip.ac.id

Keywords: thin film, Fe-doped ZnO, photodegradation, rhodamine b, methylene blue, *Escherichia coli*

OPEN ACCESS

RECEIVED
20 September 2021

REVISED
20 October 2021

ACCEPTED FOR PUBLICATION
27 October 2021

PUBLISHED
10 November 2021

Abstract

ZnO is a popular photocatalyst that is often used for the degradation of dyes and bacteria. However, the catalytic performance of ZnO is only optimal under UV light exposure. This study aims to determine the degradation performance of rhodamine b, methylene blue, and *Escherichia coli* using 0, 5, 10, 15, and 20% Fe-doped ZnO (ZnO:Fe). Deposition of thin film was carried out using the sol-gel method with a spray-coating technique, while the degradation was carried out under halogen light exposure for 3 h. The optical characterization results show that 20% Fe-doped ZnO has the highest transmittance and the lowest energy band gap of 3.21 eV based on Tauc's plot method. All thin films are hydrophilic with the largest contact angle of 68.54° by 20% Fe-doped ZnO and the lowest contact angle of 52.96° by 5% Fe-doped ZnO. The surface morphology of the thin film resembles a creeping root that is cracked and agglomerated. XRD test results show that the thin film is dominated by ZnO peaks with a wurtzite structure with a hexagonal plane phase and a crystal size of 115.5 A°. The 20% Fe-doped ZnO thin film had the most efficient degradation performance of 70.79% for rhodamine b, 65.31% for blue, and 67% for *E. coli* bacteria. Therefore, Fe-doped ZnO is a brilliant photocatalyst material that can degrade various pollutants even under visible light.

1. Introduction

Water pollution by dyes is still a big problem that has not been resolved until now [1–5]. Most of the pollution is caused by the industrial waste of clothing, fabrics, and jeans. Dyestuff waste directly discharged into the environment without being processed first becomes a source of pollution and can cause various hazards, such as toxic effects and reduced light penetration ability in waters [6, 7]. Among the various textile dyes, the most widely used are methylene blue and rhodamine b [8, 9]. In addition to dyes, water pollution by *Escherichia coli* bacteria is also a problem [10, 11]. Recently, there have been 'viral' cases of health problems caused by *Escherichia coli* contamination such as fever, typhoid, and diarrhoea experienced by residents in several districts in Indonesia, such as Banjarnegara, Gunung Kidul, and Klaten. Based on the investigation results, it was found that the water used by the community in the area contained *Escherichia coli* bacteria that exceeded the safe threshold as water that humans can consume.

The presence of dye compounds and *Escherichia coli* bacteria is a serious problem that needs proper handling. Photodegradation is one of the methods to decompose industrial waste dyes. Degradation by utilizing the aid of light offers a relatively inexpensive solution and is easy to implement in Indonesia. In operation, the principle used in this method is to activate photocatalyst materials from semiconductor materials, such as CdS, Fe_2O_3, ZnO, TiO_2, Bi_2O_3, Cu_2O, WO_3 etc [12–16]. Semiconductor materials that are easily found and most often used are TiO_2 and ZnO [17–19]. ZnO is an excellent oxidizing agent used as a photocatalyst and has a higher efficiency due to the strong absorption of UV from the solar spectrum. Compared to other catalysts, ZnO

is suitable for the detoxification process of colour waste in water because it produces H_2O_2 more efficiently [18, 20].

The photocatalytic process occurs when ZnO material in water is exposed to UV light, electrons in the valence band will be excited to the conduction band. This process produces electrons (e−) in the conduction band and holes (h^+) in the valence band. Then electrons react with oxygen molecules from water to form superoxide anion radicals (O_2^*), and holes will react with hydroxyl ions from water to form hydroxyl radical compounds (OH^*). Superoxide reacts with electrons, and H^+ ions from water form H_2O_2 compounds then react again with electrons to produce hydroxyl radicals [21]. Electrons and holes generate hydroxyl radical compounds then oxidize pollutant molecules (M) to produce degraded compounds (M′). If M is a dye such as a rhodamine b and methylene blue, M′ is dyes with a more straightforward carbon chain and lower concentration. If M is *Escherichia coli*, M′ is *Escherichia coli* with less coloni.

In fact, in the actual environment, UV levels in sunlight are microscopic. Therefore, the optical properties of ZnO need to be improved to produce electrons with visible light energy. To improve the properties of ZnO, doping with metal ions is the most effective way to produce structural changes. The optical band gap energy and ferromagnetic properties can be controlled by doping the micro conductor with a transition metal such as Fe. Fe-doped ZnO nanoparticles play an essential role in the photodegradation of organic pollutants [22] and exhibit better photocatalytic activity than undoped ZnO nanoparticles [23]. Several researchers have prepared Fe-doped ZnO nanoparticles, but high doping amounts, control of optical properties to enhance photocatalytic activity, and degradation of multianalyte are rare. In our previous study, the degradation of pollutants by Fe-doped ZnO was still using a UV excitation source [7]. In this study, the degradation was carried out under halogen rays as a representation of actual sunlight. The synthesis results were then characterized and tested for photodegradation of methylene blue, rhodamine b, and *Escherichia coli*.

2. Materials and methods

2.1. Materials

The materials used in this study were methylene blue ($C_{16}H_{18}ClN_3S$), rhodamine b ($C_{28}H_{31}N_2O_3Cl$), glass preparation, Iron Nitrate ($Fe(NO_3)_3.9H_2O$, Merck KGaA 99.95%), Zinc Acetate Dehydrate ($Zn(CH_3COO)_2.2H_2O$, Merck KGaA 97%), Acetone (Merck KGaA 99.5%), Isopropanol (Merck KGaA 99.5%), Methanol (Merck KGaA 99.9%), Aquades, Monoethanolamine (Merck KGaA), while the tools used are Mini Compressor (Krisbow, AS 186), VMC digital balance (VB 304), Degradation lamp (20 W), Hotplate Stirrer (Yellow MAG HS 7), and spray (Krisbow HS, 1200333).

2.2. Method

The Fe-doped ZnO sol-gel preparation was prepared by preparing 0.5 M zinc solution from 3.046 g $Zn(CH_3COO)_2.2H_2O$ and 26 ml isopropanol stirred with a magnetic stirrer temperature of 60 °C for 15 min until homogeneous [24]. The solution was stirred with a magnetic stirrer at 60 °C for 15 min until homogeneous. Monoethanolamine (MEA) was dropped into the solution and stirred on a hotplate at 60 °C for 15 min until the solution was colourless or transparent. Fe Nitrate with various concentrations of 0, 5, 10, 15, and 20% was mixed and then stirred for 15 min at a temperature of 60 °C. Thin film deposition was carried out using a spray-coating technique, and previously the glass substrate was cleaned using the Radio Corporation of America (RCA) method. The resulting solution is sprayed for 30 min at a temperature of 450 °C. The degradation test was carried out by making a solution of 10 ppm dye (rhodamine b and methylene blue). Photodegradation was carried out under visible light for 180 min with observations every 30 min. The degradation test of *Escherichia coli* bacteria was carried out with actual samples from the Rasamala river under visible light for 180 min.

2.3. Characterization

The morphology and chemical composition of the compounds in the thin film was observed using the Analytical Scanning Electron Microscopy—Energy Dispersive x-ray instrument (SEM—EDX JEOL JSM-6510LA). Analysis of the thin film crystallinity using x-ray Diffraction instrument (Shimadzu Maxima XRD-700). Determination of the contact angle of the tips film using a digital microscope endoscope camera instrument. Optical characteristics and efficiency photodegradation of dyes and *Escherichia coli* were analyzed based on the results of the UV–vis Spectrophotometer (Shimadzu UV–vis 1240 SA).

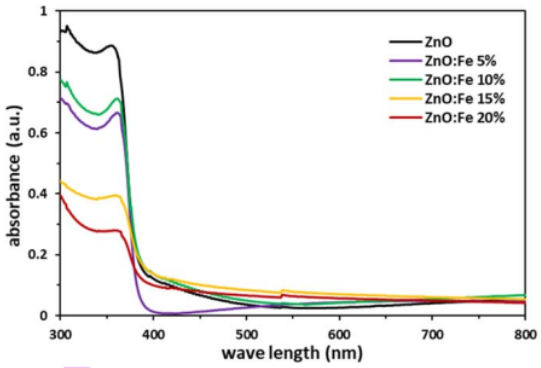

Figure 1. The absorbance spectrum of the Fe-doped ZnO thin film.

Table 1. Fe-doped ZnO thin film contact angle against rhodamine b and methylene blue.

	Contact angle (°)	
Thin film	Rhodamin b	Methylene blue
Undoped ZnO	62.53	63.27
5% Fe-doped ZnO	52.96	57.62
10% Fe-doped ZnO	55.55	61.81
15% Fe-doped ZnO	65.75	62.83
20% Fe-doped ZnO	66.89	68.54

3. Results and discussion

The optical properties of the Fe-doped ZnO thin film obtained from the UV–vis test are shown by transmittance and absorbance graphs. Tests of the absorbance spectrum of Fe-doped ZnO thin film in the wavelength range of 300–800 nm are shown in figure 1. The highest transmittance is by 20% Fe-doped ZnO thin film at the same wavelength, while the highest absorbance is undoped ZnO. Substitution of Zn atoms by Fe atoms will form close distances between particles with less light [25]. It indicates that the concentration of Fe is very influential with the transmittance value because it can produce a different number of electron-hole pairs for each sample. The less Fe, the fewer electrons are produced so that the photon energy absorbed by the electrons to be also excited less and the transmittance value is increased.

The energy band gap value is processed using Tauc's plot method as shown at figure 2. In this study, the shift that occurs is redshift, as shown from the results of 0%–20% Fe-doped ZnO, namely 3.32, 3.28, 3.25, 3.21, and 3.21 eV. This result is consistent with the study reported by Ariyakkani *et al* (2017) for Fe-doped ZnO thin films, where the Eg value decreased from 3.38 eV for undoped ZnO to 3.07 eV for 20% Fe-doped ZnO [26]. A decrease in the energy bandgap indicates the shift that occurs as the concentration of Fe increases. Thus, the decrease in the energy bandgap occurs because the valence electrons of Fe larger than Zn will cause Fe to become a donor atom near the conduction band so that the electron transition requires less energy to the conduction band [27, 28]. The decrease in the energy band gap value can also be explained by the presence of Fe atoms in ZnO can suppress crystal growth. In addition, the inclusion of Fe in ZnO also causes defects in ZnO crystals that cause high light absorption, which is very necessary to increase the photoactivity of visible light from ZnO [29].

The hydrophilicity test was carried out between the dye solution and the surface of the film that had been coated on a glass plate using a Contact Anglemeter. Table 1 shows all the Fe-doped ZnO films forming a contact angle of less than 90° which means the films can interact well with water. Despite being dropped with two different dyes (rhodamine b and methylene blue), the resulting contact angle increased uniformly as the Fe concentration in ZnO increased, from 62.53° to 66.89° and 63.27° to 68.54°. This result is in contrast to ZnO doped with other materials, such as La, Na, Pb, and Mg, where the addition of a doping concentration of less than 7.5% reduces the contact angle value [30, 31], including our previous study where the addition of Fe also lowers the value of the contact angle [7].

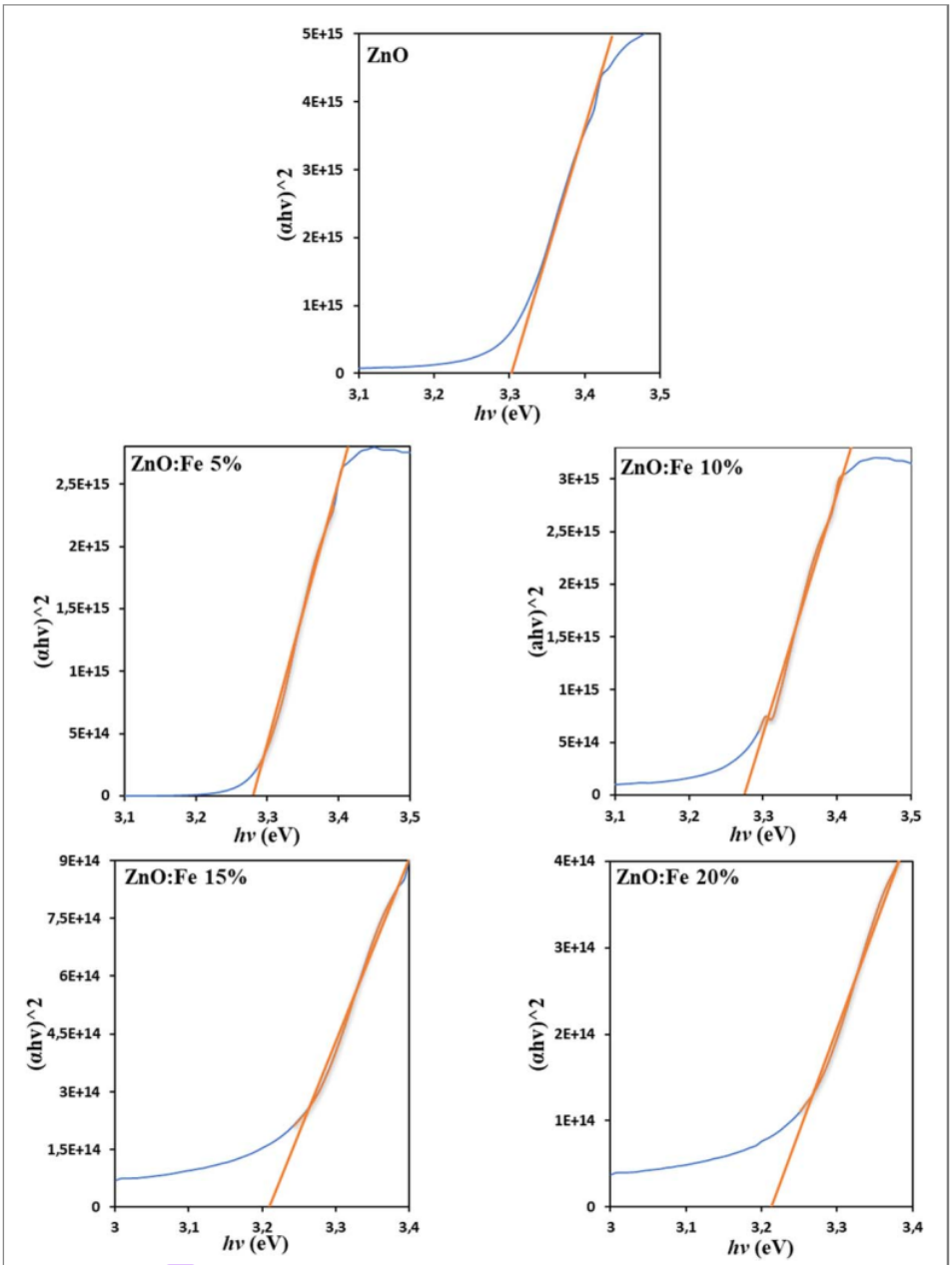

Figure 2. The energy band gap of Fe-doped ZnO thin film using Tauc's plot method.

Interestingly, these results indicate that the addition of Fe doping less than 10% will increase the hydrophilic properties, while the addition of Fe doping more than 10% will increase the hydrophobic properties. This change in properties is probably due to differences in the microstructure and morphology of each doped film. Changes in properties that lead to an increase in hydrophobic properties will be advantageous for degradation applications because it increases the surface area and causes an increase in analyte adsorption on the catalyst surface [32]. The higher the contact angle formed by the thin film, the higher the degradation efficiency produced under halogen light.

SEM characterization is needed to determine the material's physical properties, including its microstructure and surface morphology. Figure 3 shows the results of Fe-doped ZnO thin film characterization using SEM with

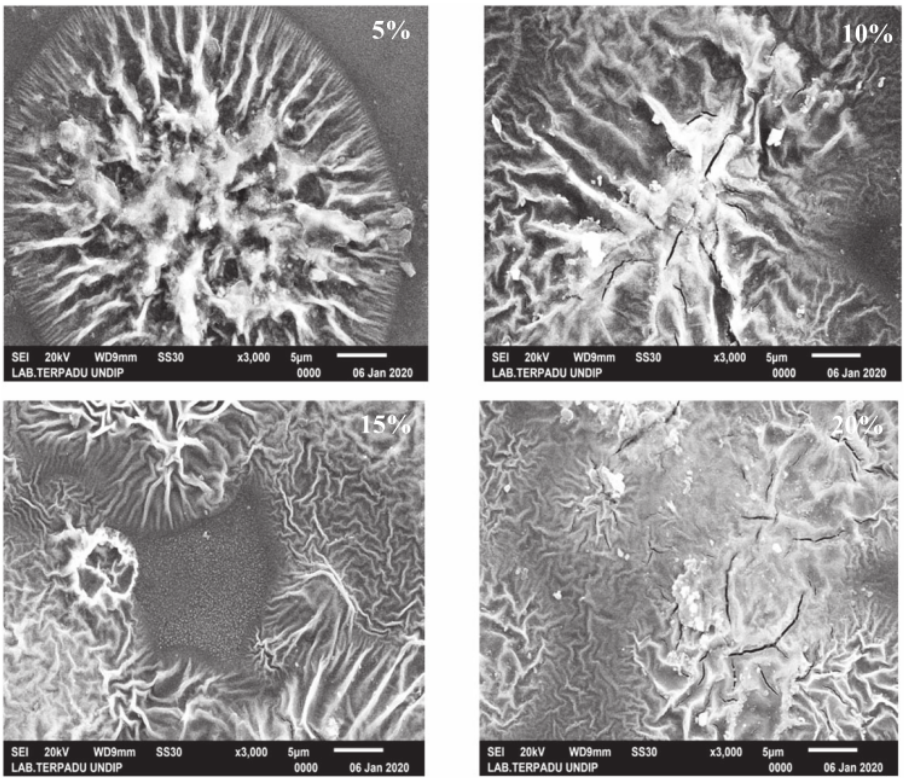

Figure 3. Surface morphology of Fe-doped ZnO thin film 3000× magnification.

3000× magnification. Fe-doped ZnO thin film appears to have a root-like morphology grouped and evenly distributed over the entire substrate surface. The root-like surface morphology is caused by the bonds between the particles deposited in the presence of high temperatures on the substrate. These bonds result in the grains becoming fused and forming a structure that looks like a root [33]. The diameter of the size formed ranged from 150 nm to 500 nm with an average particle size of 333.75 nm. A high concentration of Fe dopant resulted in the appearance of agglomeration and aggregation in ZnO morphology [34], also causing irregular cracked surfaces.

Characterization using EDX is needed to determine the chemical properties, including the material's elemental composition. Table 2 show that O, Fe, and Ze atoms were successfully formed on the substrate. The increase in the percentage of mass and Fe atoms and the increase in the number of concentrations. It indicates an increase in the molecules that make up the thin film formed. It causes the resulting energy band gap to become smaller, and the ability of Fe-doped ZnO to photodegrade in the visible light spectrum is getting better. X-ray diffraction test results were carried out to determine the phase contained in the sample. From the results of the XRD test, analysis was carried out by matching the spectrum of the XRD test results with JCPDS data (Joint Committee on Powder Diffraction Standard) which helps know what compounds are contained in the Fe-doped ZnO. JCPDS data used are JCPDS 36–1451 (ZnO), JCPDS 06-0696 (Fe), and JCPDS 24-0072 (Fe_2O_3). Figure 4 shows the XRD test results for 20% Fe-doped ZnO showing several diffraction peaks with the most dominant peak belonging to ZnO with 2θ used between 20°–90° and the wavelength used =1.5405 Å.

The XRD test results showed that the ZnO sample had a wurtzite structure with hexagonal plane phases showed that the diffraction peaks were at $2\theta = 31.76°$, 34.26°, 36.10°, 47.48°, 56.54°, 62.90°, and 67.82° with Miller indices (100), (002), (101), (102), (110), (103), and (200) [35–37]. This result is similar with the study reported by Roguai and Djelloul (2021), where all the peaks of the XRD spectrum (100), (002), (101), (102), (110), (103), and (200) for Fe-doped ZnO (0%–10%) are identified as single-phase ZnO wurtzite structure with the space group $P6_3mc$ [38]. During synthesis, the doping addition of ferrite nitrate led to a peak at 24.22°, corresponding to (012) Fe_2O_3 [39]. In the hexagonal structure, lattice constants (a and c), unit cell volume (V), crystal size (D), lattice strain (ε), and atomic packing fraction (APF) are calculated using the following formula [40]:

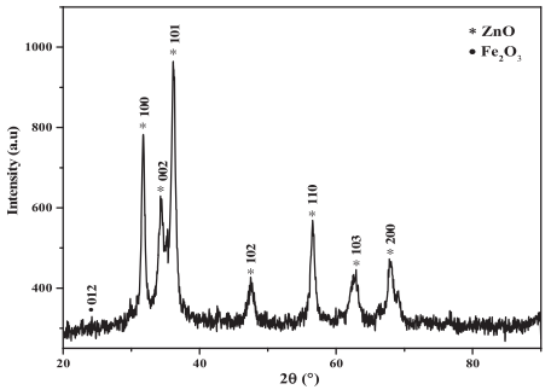

Figure 4. XRD results of 20% Fe-doped ZnO thin film.

Table 2. The mass composition of the chemical elements Fe-doped ZnO thin film.

	Mass of Fe-doped ZnO (%)			
Element	5%	10%	15%	20%
O	49.03	54.96	58.38	53.31
Fe	2.05	3.41	3.58	5.47
Zn	48.92	41.63	38.04	41.21

Table 3. Crystal parameters of Fe-doped ZnO.

Parameter	Value	Unit
a	1.509586	Å
c	1.57997	Å
V	3.118137	Å^3
APF	1.154747	%

$$a = \frac{\lambda}{\sqrt{3}\ \sin\theta_{(100)}} \tag{1}$$

$$c = \frac{\lambda}{\sqrt{3}\ \sin\theta_{(002)}} \tag{2}$$

$$V = \frac{\sqrt{3}}{2}a^2c \tag{3}$$

$$APF = \frac{2\pi}{3\sqrt{3}}\frac{a}{c} \tag{4}$$

The results of calculations using the formulas (1) to (5) are shown in table 3 below:

X-ray diffraction is also used to determine the Crystal Size (D) by using the Debye Sherrer equation approach as follows:

$$D = \frac{K\ \lambda}{\beta\ \cos\theta} \tag{5}$$

Where is the wavelength of x-rays (1.54056) and is the value of Full Width at Half Maximum (FWHM), and K is the crystal form factor whose values are between 0.9. The Debye–Scherrer equation is then modified into equation (6) as follows:

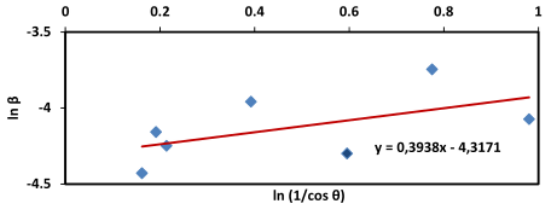

Figure 5. Relationship chart of ln $(1/\cos\theta)$ versus ln β.

Table 4. Calculation of (ln $1/\cos\theta$) and (ln β).

2θ	Crystal plane orientation	$1/\cos\theta$	β (*rad*)	ln $1/\cos\theta$	ln β
31.76	100	1.1758	0.01193	0.16195	−4.42894425
34.26	002	1.21092	0.01564	0.19138	−4.1582305
36.10	101	1.23844	0.01427	0.21385	−4.24943083
47.48	102	1.4805	0.01908	0.39238	−3.95921498
56.54	110	1.8134	0.01358	0.59521	−4.29944439
62.90	103	2.17099	0.02362	0.77518	−3.74586958
67.82	200	2.66511	0.017	0.98025	−4.07475961

$$\ln\beta = \ln\frac{K\lambda}{D} + \ln\frac{1}{\cos\theta} \tag{6}$$

The calculation of the values (ln $1/\cos$) and (ln) XRD analysis results in all crystal plane orientations are shown in figure 5 and table 4:

The value of intercept from the graph of the relationship ln $(1/\cos)$ as the *x*-axis and ln as the *y* axis is equal to $((K)/D)$, so equation (6) can be modified into the following equation:

$$D = \frac{K\lambda}{\exp(y_0)} \tag{7}$$

Where y_0 is the intercept value of the graph ln $(1/\cos)$ versus ln, the intercept value from the graph above is −4.3171, so the crystal size is 115.5 A°. This result may be the smallest crystal size among other samples not tested, considering that several previous studies increasing the Fe content reduced the lattice parameters and the average crystal size [34, 41, 42].

Figure 6 and table 5 show the results of the photodegradation carried out to test the photocatalyst activity of Fe-doped ZnO. Photocatalyst activity was tested to degrade rhodamine b, methylene blue, and *Escherichia coli* under halogen to represent visible light. Photocatalyst reactions that occur in the reaction of Fe-doped ZnO material with visible light can excite electrons and leave holes [43, 44]. The electrons interact with the oxygen present in the water to produce superoxide. Meanwhile, hydroxyl radicals are generated from the interaction between holes and water. Hydroxyl radicals are potent oxidizing agents, so they are capable of oxidizing organic compounds. The radicals formed will break down the dye molecules to produce H_2O and CO_2 [45].

Photodegradation of the thin film under visible light for rhodamine b and methylene blue degradation based on 5%–20% Fe-doped ZnO, are 64.53; 65.57; 67.36; 70.79% and 60.64; 62.53; 62.34; 65.31%. The photodegradation of *Escherichia coli* was 25, 42, 50, and 67%. The most optimal degradation ability is possessed by a 20% Fe-doped ZnO, both on rhodamine b, methylene blue, and *Escherichia coli*. The energy band gap value influences the effectiveness of the photocatalyst thin film performance. The small energy band gap indicates that the energy required to excite electrons from the valence band to the conduction band is getting smaller. With the same amount of energy, a thin film with a small energy band gap can produce more electron-hole pairs than a thin film with a large energy bandgap. Therefore, the smaller the energy band gap, the higher the degradation ability under visible light. On the other hand, the larger the energy band gap, the lower the degradation ability under visible light.

The presence of Fe found in EDX measurements is believed to form a trapping state between the conduction band and the valence band, which can inhibit the recombination rate of electron and hole pairs and increase photocatalytic activity. This result was confirmed by Bousslama *et al* (2017), who investigated Fe-doped ZnO for the degradation of rhodamine b [28], Saleh and Djaja (2014) for the degradation of methyl orange [46], and

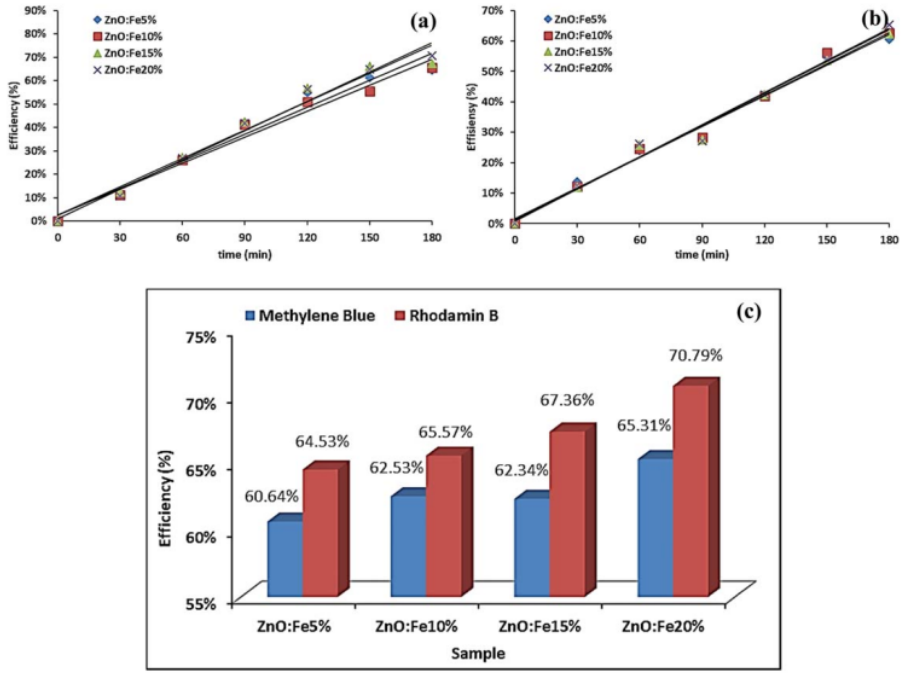

Figure 6. (a) Photodegradation of rhodamine b (b) photodegradation of methylene blue (c) photodegradation efficiency diagram of e-doped ZnO under visible light.

Table 5. Bacterial degradation test results.

Thin film	Degradation efficiency (%)
5% Fe-doped ZnO	25
10% Fe-doped ZnO	42
15% Fe-doped ZnO	50
20% Fe-doped ZnO	67

Roguai and Djelloul (2021) for the degradation of methylene blue [38]. Fe^{2+} and Fe^{3+} ions obtained are known to form 2 new energy levels in the energy gap. One energy level is above the valence band, which refers to the 3d orbital of Fe^{3+}, and the other is below the conduction band because the electron energy level of the Fe^{2+} ion is lower than the 3d Zn in the conduction band [25, 46].

When halogen light is given, electrons can be excited from Fe^{3+} and the valence band to the conduction band. After the electrons are excited, Fe^{3+} will be converted to Fe^{4+}, which can interact with hydroxyl ions and produce OH hydroxyl radicals. Simultaneously, electrons excited to the valence band can react with oxygen and produce superoxide radicals (O_2^*). The formed active radical species will initiate a series of redox processes to break down dye compounds into simpler ones and cause *Escherichia coli* cell membranes to lyse. Therefore, developing a thin film with appropriate optical properties such as 20% Fe-doped ZnO would be advantageous for the degradation of liquid pollutants since electron-hole pairs can be generated only by a visible light excitation source.

4. Conclusions

The increase in Fe dopant impacts improving optical properties, decreasing the energy bandgap and increasing the photocatalytic properties of ZnO thin films. A Fe-doped ZnO thin film has a root-like surface morphology dominated by ZnO peaks with a wurtzite structure with a hexagonal plane. Fe dopant determines the hydrophilicity of film, and the magnitude of the contact angle is directly proportional to the degradation

efficiency. 20% Fe-doped ZnO is the best photocatalyst thin film formula for degrading dyes and *Escherichia coli* under visible light.

Acknowledgments

We want to thank the Ministry of Research, Technology, and Higher Education Indonesian for supporting research funding (PDUPT No. 257-59/UN7.6.1/PP/2021).

Data availability statement

All data that support the findings of this study are included within the article (and any supplementary files).

ORCID iDs

Heri Sutanto https://orcid.org/0000-0001-7119-9633
Ilham Alkian https://orcid.org/0000-0002-2386-0252

References

[1] Lops C, Ancona A, Di Cesare K, Dumontel B, Garino N, Canavese G and Cauda V 2019 Sonophotocatalytic degradation mechanisms of Rhodamine B dye via radicals generation by micro- and nano-particles of ZnO *Appl. Catalysis* B **243** 629–40
[2] Nguyen C H, Fu C C and Juang R S 2018 Degradation of methylene blue and methyl orange by palladium-doped TiO_2 photocatalysis for water reuse: efficiency and degradation pathways *J. Clean. Prod.* **202** 413–27
[3] Pang Y, Ruan Y, Feng Y, Diao Z, Shih K, Chen D and Kong L 2019 Ultrasound assisted zero valent iron corrosion for peroxymonosulfate activation for Rhodamine-B degradation *Chemosphere* **228** 412–7
[4] Pratiwi N I, Sari S R, Arifan F, Wulandari A T, Alkian I, Mustasjar B and Aji M B F B 2020 Batik pemalang organic wastewater composition and simple electrocoagulation-filtration treatment *IOP Conf. Ser.: Earth Environ. Sci.* vol 448 (Bristol: IOP Publishing) p 012055
[5] Larasati D A, Alkian I, Arifan F and Sari S R 2020 Batik home industry wastewater treatment using UVC/ozon oxidation method: case study in Cibelok Village, Pemalang, Indonesia *IOP Conf. Ser.: Earth Environ. Sci.* vol 448 (Bristol: IOP Publishing) p 012055
[6] Arshad H M U, Anwar H, Javed Y, Naz M Y, Ghaffar A, Khan M Z and Farooq Z 2019 Investigation of photocatalytic degradation of methylene orange dye using titanium dioxide–zinc oxide nanocomposites *Mater. Res. Express* **6** 125009
[7] Sutanto H, Alkian I, Pramunditya V J, Mukholit M, Hidayanto E, Duri I R and Priyono 2020 Effect of Fe addition an ZnO thin films for photodegradation under UV and halogens light *International Journal of Scientific & Technology Research* **9** 315–8
[8] Suharyadi E, Muzakki A, Nofrianti A, Istiqomah N I, Kato T and Iwata S 2020 Photocatalytic activity of magnetic core–shell $CoFe_2O_4$@ZnO nanoparticles for purification of methylene blue *Mater. Res. Express* **7** 085013
[9] Sun Y, Gao Y, Zhao B, Xu S, Luo C and Zhao Q 2020 One-step hydrothermal preparation and characterization of ZnO–TiO_2 nanocomposites for photocatalytic activity *Mater. Res. Express* **7** 085010
[10] Wang W, Zeng Z, Zeng G, Zhang C, Xiao R, Zhou C and Zhou Y 2019 Sulfur doped carbon quantum dots loaded hollow tubular g-C_3N_4 as novel photocatalyst for destruction of *Escherichia coli* and tetracycline degradation under visible light *Chem. Eng. J.* **378** 122132
[11] Syahrul F, Wahyuni C U, Notobroto H B, Wasito E B, Adi A C and Dwirahmadi F 2020 Transmission media of foodborne diseases as an index prediction of diarrheagenic *Escherichia coli*: study at elementary school, Surabaya, Indonesia *International Journal of Environmental Research and Public Health* **17** 8227
[12] Cheng L, Xiang Q, Liao Y and Zhang H 2018 CdS-based photocatalysts *Energy Environ. Sci.* **11** 1362–91
[13] Hitam C N C and Jalil A A 2020 A review on exploration of Fe_2O_3 photocatalyst towards degradation of dyes and organic contaminants *J. Environ. Manage.* **258** 110050
[14] Poorsajadi F, Sayadi M H, Hajiani M and Rezaei M R 2020 Synthesis of CuO/Bi_2O_3 nanocomposite for efficient and recycling photodegradation of methylene blue dye *Int. J. Environ. Anal. Chem.* 1–14
[15] Bouallouche R, Dalhatou S, Kane A, Nasrallah N, Hachemi M, Amrane A and Assadi A A 2021 Reconsideration of the contribution of photogenerated ROS in methyl orange degradation on TiO_2, Cu_2O, WO_3, and Bi_2O_3 under low-intensity simulated solar light: mechanistic understanding of photocatalytic activity *Euro-Mediterranean Journal for Environmental Integration* **6** 1–10
[16] Borade P A, Suroshe J S, Bogale K, Garje S S and Jejurikar S M 2020 Photocatalytic performance of ZnO carbon composites for the degradation of methyl orange dye *Mater. Res. Express* **7** 015512
[17] Sakthivel S, Neppolian B, Shankar M, Arabindoo B, Palanichamy M and Murugesan V 2003 Solar photocatalytic degradation of azo dye: comparison of photocatalytic efficiency of ZnO and TiO_2 *Sol. Energy Mater. Sol. Cells* **77** 65–82
[18] Bica B O and de Melo J V S 2020 Concrete blocks nano-modified with zinc oxide (ZnO) for photocatalytic paving: performance comparison with titanium dioxide (TiO_2) *Constr. Build. Mater.* **252** 119120
[19] Hidayanto E, Sutanto H, Wibowo S and Irwanto M 2017 Morphology and degradation kinetics of N-doped TiO_2 nanoparticle synthesized using sonochemical method *Solid State Phenomena* **266** 95–100
[20] Shah A A, Chandio A D and Sheikh A A 2021 Boron doped ZnO nanostructures for photo degradation of methylene blue, methyl orange and rhodamine B *J. Nanosci. Nanotechnol.* **21** 2483–94
[21] Sutanto H, Wibowo S, Nurhasanah I, Hidayanto E and Hadiyanto H 2016 Ag doped ZnO thin films synthesized by spray coating technique for methylene blue photodegradation under UV irradiation *International Journal of Chemical Engineering* **2016** 1–6
[22] Ba-Abbad M M, Kadhum A A H, Mohamad A B, Takriff M S and Sopian K 2013 Visible light photocatalytic activity of Fe^{3+}-doped ZnO nanoparticle prepared via sol–gel technique *Chemosphere* **91** 1604–11

[23] Hui A, Ma J, Liu J, Bao Y and Zhang J 2017 Morphological evolution of Fe doped sea urchin-shaped ZnO nanoparticles with enhanced photocatalytic activity *J. Alloys Compd.* **696** 639–47
[24] Sutanto H, Hidayanto E, Irwanto M and Wibowo S 2017 The influence of nitrogen doping concentration on the strain and band gap energy of N-doped zinc oxide prepared using spray coating technique *Solid State Phenomena* **266** 141–7
[25] Dong S, Xu K, Liu J and Cui H 2011 Photocatalytic performance of ZnO:Fe array films under sunlight irradiation *Physica* B **406** 3609–12
[26] Ariyakkani P, Suganya L and Sundaresan B 2017 Investigation of the structural, optical and magnetic properties of Fe doped ZnO thin films coated on glass by sol-gel spin coating method *J. Alloys Compd.* **695** 3467–75
[27] Cheng W and Ma X 2009 Structural, optical and magnetic properties of Fe-doped ZnO *J. Phys. Conf. Ser.* vol 152 (Bristol: IOP Publishing) p 012039
[28] Bousslama W, Elhouichet H and Férid M 2017 Enhanced photocatalytic activity of Fe doped ZnO nanocrystals under sunlight irradiation *Optik* **134** 88–98
[29] Sze-Mun L, Jin-Chung S, Honghu Z, Hua L, Haixiang L, Yen-Yi C, Man-Kit C and Abdul R M 2021 Green synthesis of Fe–ZnO nanoparticles with improved sunlight photocatalytic performance for polyethylene film deterioration and bacterial inactivation *Mater. Sci. Semicond. Process.* **123** 105574
[30] Shaban M and El Sayed A 2016 Effects of Lanthanum and sodium on the structural, optical and hydrophilic properties of sol-gel derived ZnO films: a comparative study *Material Science in Semiconductor Processing* **41** 323–34
[31] Shaban M and El Sayed A M 2015 Influences of lead and magnesium Co-doping on the nanostructural, optical properties and wettability of spin coated zinc oxide films *Mater. Sci. Semicond. Process.* **39** 136–47
[32] Najafidoust A, Asl E A, Hakki H K, Sarani M, Bananifard H, Sillanpaa M and Etamadi M 2021 Sequential impregnation and sol-gel synthesis of Fe-ZnO over hydrophobic silica aerogel as a floating photocatalyst with highly enhanced photodecomposition of BTX compounds from water *Sol. Energy* **225** 334–56
[33] Sutanto H, Durri S, Wibowo S, Hadiyanto H and Hidayanto E 2016 Root-like morphology of Zno: Al thin film deposited on amorphous glass substrate by sol-gel method *Physics Research International* **2016** 1–7
[34] Kumar M S and Arunagiri C 2021 Efficient photocatalytic degradation of organic dyes using Fe-doped ZnO nanoparticles *J. Mater. Sci., Mater. Electron.* **32** 17925–35
[35] Liu Q, Dai J, Hu F, Zhang Z, Xiong K and Xu G 2021 Core–shell structured Fe/ZnO composite with superior electromagnetic wave absorption performance *Ceram. Int.* **47** 14506–14
[36] Ciciliati M A, Silva M F, Fernandes D M, de Melo M A C, Hechenleitner A A W and Pineda E A G 2015 Fe-doped ZnO nanoparticles: synthesis by a modified sol–gel method and characterization *Material Letter* **159** 84–6
[37] Basyooni M A, Shaban M and El Sayed A M 2017 Enhanced gas sensing properties of spin-coated Na-doped ZnO nanostructured films *Sci. Rep.* **7** 1–12
[38] Roguai D and Djelloul P 2021 Structural, microstructural and photocatalytic degradation of methylene blue of zinc oxide and Fe-doped ZnO nanoparticles prepared by simple coprecipitation method *Solid State Commun.* **334–335** 1–9
[39] Mohammadigharehbagh R, Pat S, Akkurt N and Korkmaz S 2021 Studies on the morphological, structural, optical and electrical properties of Fe-doped ZnO magnetic nano-crystal thin films *Physica B: Physics of Condensed Matter* **609** 412921
[40] Monshi A, Mohammad R F and Mohammad R M 2012 Modified Scherrer equation to estimate more accurately nano-crystallite size using XRD *World Journal of Nano Science and Engineering* **2** 154–60
[41] Pakizeh E 2020 Optical response and structural properties of Fe-doped $Pb(Zr0.52Ti0.48)O_3$ nanopowders *J. Mater. Sci., Mater. Electron.* **31** 4872–81
[42] Saadi H, Rhouma F I H, Benzarti Z, Bougrioua Z, Guermazi S and Khirouni K 2020 Electrical conductivity improvement of Fe doped ZnO nanopowders *Mater. Res. Bull.* **129** 110884–90
[43] Srivastava A, Kumar N and Khare S 2014 Enhancement in UV emission and band gap by Fe doping in ZnO thin films *Opto-Electron. Rev.* **22** 68–76
[44] Khalid N R, Hammad A, Tahir M B, Rafique M, Iqbal T, Nabi G and Hussain M K 2019 Enhanced photocatalytic activity of Al and Fe co-doped ZnO nanorods for methylene blue degradation *Ceram. Int.* **45** 21430–5
[45] Xu L and Li X 2010 Influence of Fe-doping on the structural and optical properties of ZnO thin films prepared by sol–gel method *J. Cryst. Growth* **312** 851–5
[46] Saleh R D and Febiana N 2014 UV light photocatalytic degradation of organic dyes with Fe-doped ZnO nanoparticles *Superlattices Microstruct.* **74** 217–33

Analysis of Fe-doped ZnO thin films for degradation of rhodamine B, methylene blue, and Escherichia coli under visible light

ORIGINALITY REPORT

20%	8%	16%	5%
SIMILARITY INDEX	INTERNET SOURCES	PUBLICATIONS	STUDENT PAPERS

PRIMARY SOURCES

1	Submitted to Higher Education Commission Pakistan Student Paper	2%
2	Rosari Saleh, Nadia Febiana Djaja. "UV light photocatalytic degradation of organic dyes with Fe-doped ZnO nanoparticles", Superlattices and Microstructures, 2014 Publication	2%
3	Zohra Nazir Kayani, Eram Abbas, Zeb Saddiqe, Saira Riaz, Shahzad Naseem. "Photocatalytic, antibacterial, optical and magnetic properties of Fe-doped ZnO nano-particles prepared by sol-gel", Materials Science in Semiconductor Processing, 2018 Publication	1%
4	Submitted to Universitas Diponegoro Student Paper	1%
5	Lis Permana Sari, Zuhdi Saputro, Maximus Pranjoto Utomo, Anti Kolonial Prodjosantoso.	1%

"The Use of Salacca Zalacca Extract as Reducing Agent to Synthesize Silver Nanoparticles (Agnps) and the Antibacterial Activities.", Oriental Journal Of Chemistry, 2019
Publication

---

6 A. Goktas, I.H. Mutlu, Y. Yamada. "Influence of Fe-doping on the structural, optical, and magnetic properties of ZnO thin films prepared by sol–gel method", Superlattices and Microstructures, 2013 — 1 %
Publication

---

7 www.hindawi.com — 1 %
Internet Source

---

8 www.tandfonline.com — 1 %
Internet Source

---

9 C. Aydın, M.S. Abd El-sadek, Kaibo Zheng, I.S. Yahia, F. Yakuphanoglu. "Synthesis, diffused reflectance and electrical properties of nanocrystalline Fe-doped ZnO via sol–gel calcination technique", Optics & Laser Technology, 2013 — 1 %
Publication

---

10 Cheng-Kuo Tsai, Yu-Chin Lee, Thanh Tam Nguyen, Jao-Jia Horng. "Levofloxacin degradation under visible-LED photo-catalyzing by a novel ternary Fe–ZnO/WO3 nanocomposite", Chemosphere, 2022 — <1 %

	Publication	
11	opus.lib.uts.edu.au Internet Source	<1 %
12	www.ncbi.nlm.nih.gov Internet Source	<1 %
13	Shuo Wang, Zhenke Chen, Ying Zhao, Chenlu Sun, Jianye Li. "High Photocatalytic Activity over Starfish-like La-doped ZnO/SiO2 Photocatalyst for Malachite Green Degradation under Visible Light", Journal of Rare Earths, 2020 Publication	<1 %
14	link.springer.com Internet Source	<1 %
15	www.jmrt.com.br Internet Source	<1 %
16	Submitted to The University of Manchester Student Paper	<1 %
17	onlinelibrary.wiley.com Internet Source	<1 %
18	Ackmez Mudhoo, Sonam Paliya, Prittam Goswami, Mukesh Singh et al. "Fabrication, functionalization and performance of doped photocatalysts for dye degradation and mineralization: a review", Environmental Chemistry Letters, 2020	<1 %

Publication

19	Bingqing Zhang, Jingying Shi, Chunmei Ding, Ruifeng Chong et al. "Conversion of Biomass Derivatives to Electricity in Photo Fuel Cells using Undoped and Tungsten-doped Bismuth Vanadate Photoanodes", ChemSusChem, 2015 Publication	<1 %
20	cst.kipmi.or.id Internet Source	<1 %
21	Christian Belgardt, Harald Graaf, Thomas Baumgärtel, Christian von Borczyskowski. "Self‐assembled monolayers on silicon oxide", physica status solidi c, 2010 Publication	<1 %
22	Wiem Bousslama, Habib Elhouichet, Mokhtar Férid. "Enhanced photocatalytic activity of Fe doped ZnO nanocrystals under sunlight irradiation", Optik - International Journal for Light and Electron Optics, 2017 Publication	<1 %
23	Yan Bao, Caiping Feng, Cheng Wang, Jianzhong Ma, Chenchen Tian. "Hygienic, antibacterial, UV-shielding performance of polyacrylate/ZnO composite coatings on a leather matrix", Colloids and Surfaces A: Physicochemical and Engineering Aspects, 2017	<1 %

Publication

24	Anindita Samanta, M.N. Goswami, P.K. Mahapatra. "Fe-doped ZnO nanoparticles as novel photonic and multiferroic semiconductor", Materials Chemistry and Physics, 2020 Publication	<1 %
25	Faheem Ahmed, Shalendra Kumar, Nishat Arshi, M. S. Anwar, Bon Heun Koo. "Morphological evolution between nanorods to nanosheets and room temperature ferromagnetism of Fe-doped ZnO nanostructures", CrystEngComm, 2012 Publication	<1 %
26	Submitted to SASTRA University Student Paper	<1 %
27	aip.scitation.org Internet Source	<1 %
28	www.researchgate.net Internet Source	<1 %
29	Ahmad Najafidoust, Ebrahim Abbasi Asl, Hamid Kazemi Hakki, Mina Sarani, Hamed Bananifard, Mika Sillanpaa, Mehdi Etemadi. "Sequential impregnation and sol-gel synthesis of Fe-ZnO over hydrophobic silica aerogel as a floating photocatalyst with highly	<1 %

enhanced photodecomposition of BTX compounds from water", Solar Energy, 2021
Publication

30	Gaurav Madhu, Dev K. Mandal, Haripada Bhunia, Pramod K. Bajpai. "Thermal degradation kinetics and lifetime of HDPE/PLLA/pro-oxidant blends", Journal of Polymer Engineering, 2016 Publication	<1 %
31	cdmf.org.br Internet Source	<1 %
32	www.research.manchester.ac.uk Internet Source	<1 %
33	Anca-Ionela Istrate, Florin Nastase, Iuliana Mihalache, Florin Comanescu et al. "Synthesis and characterization of Ca doped ZnO thin films by sol–gel method", Journal of Sol-Gel Science and Technology, 2019 Publication	<1 %
34	Heri Sutanto, Singgih Wibowo, Hadiyanto, Mohammad Arifin, Eko Hidayanto. "Photocatalytic activity of cobalt-doped zinc oxide thin film prepared using the spray coating technique", Materials Research Express, 2017 Publication	<1 %

35	Lee, Kian Mun, Chin Wei Lai, Koh Sing Ngai, and Joon Ching Juan. "Recent developments of zinc oxide based photocatalyst in water treatment technology: A review", Water Research, 2016. Publication	<1 %
36	Manpreet Kaur, Vishesh Kumar, Prabhsharan Kaur, Madan Lal, Puneet Negi, Rakesh Sharma. "Effect on the dielectric properties due to In–N co-doping in ZnO particles", Journal of Materials Science: Materials in Electronics, 2021 Publication	<1 %
37	Suat Pat, Özer Çelik, Alper Odabaş, Şadan Korkmaz. "Optical properties of Nb2O5 doped ZnO nanocomposite thin film deposited by thermionic vacuum arc", Optik, 2022 Publication	<1 %
38	Wang, C.. "Structure, morphology and properties of Fe-doped ZnO films prepared by facing-target magnetron sputtering system", Applied Surface Science, 20090515 Publication	<1 %
39	cyberleninka.org Internet Source	<1 %
40	maglab.iphy.ac.cn Internet Source	<1 %

41	ouci.dntb.gov.ua Internet Source	<1%
42	www.intechopen.com Internet Source	<1%
43	A A Fogarasy. "The influence of manufacturing tolerances on the kinematic performance of mechanisms", Proceedings of the Institution of Mechanical Engineers Part C Journal of Mechanical Engineering Science, 01/01/1998 Publication	<1%
44	Ariyakkani, Premalatha, Suganya Lakshmikanthan, and Sundaresan Balakrishnan. "Investigation of the structural, optical and magnetic properties of Fe doped ZnO thin films coated on glass by sol-gel spin coating method", Journal of Alloys and Compounds, 2016. Publication	<1%
45	S. Aiswarya Devi, M. Harshiny, S. Udaykumar, P. Gopinath, M. Matheswaran. "Strategy of metal iron doping and green-mediated ZnO nanoparticles: dissolubility, antibacterial and cytotoxic traits", Toxicology Research, 2017 Publication	<1%
46	V. Chaitra. "Surface, structural and optical analysis of Fe doped nanocrystalline ZnO	<1%

films as transducer", International Conference on Nanoscience Engineering and Technology (ICONSET 2011), 11/2011

Publication

Exclude quotes	Off	Exclude matches	Off
Exclude bibliography	On		